

Quantum logic gates for capacitively coupled Josephson junctions

Frederick W. Strauch, Philip R. Johnson, Alex J. Dragt, C. J. Lobb, J. R. Anderson, and F. C. Wellstood
 Department of Physics, University of Maryland,
 College Park, Maryland 20742-4111
 (Dated: March 26, 2019)

Based on a quantum analysis of two capacitively coupled current-biased Josephson junctions, we propose two fundamental two-qubit quantum logic gates. Each of these gates, when supplemented by single-qubit operations, is sufficient for universal quantum computation. Numerical solutions of the time-dependent Schrödinger equation demonstrate that these operations can be performed with good fidelity.

PACS numbers: 74.50.+r, 03.67.Lx, 85.25.Cp

Keywords: Qubit, quantum computing, superconductivity, Josephson junction.

The current-biased Josephson junction is an easily fabricated superconducting device with great promise as a scalable solid-state qubit [1], as demonstrated by the recent observations of Rabi oscillations by Martinis et al. [2] and Yu et al. [3]. Single-qubit operations in this system can be performed through manipulation of the bias currents and application of microwave pulses resonant with the energy level splitting [2].

In this Letter, we analyze the quantum dynamics of two capacitively coupled current-biased Josephson junctions. We identify two quantum logic gates that, together with single-qubit operations, provide all necessary ingredients for a universal quantum computer. We perform full dynamical simulations of these gates through numerical integration of the time-dependent Schrödinger equation. These two-qubit operations may be experimentally probed with the methods already used to observe single junction Rabi oscillations [2, 3]. Such experiments are of fundamental importance: the successful demonstration of macroscopic quantum entanglement holds profound implications for the universal validity of quantum mechanics [4]. Finally, our methods are applicable to the alternative promising superconducting proposals based on charge [5], flux [6], and hybrid realizations [7].

Figure 1(a) shows the circuit diagram of our coupled qubits. Each junction has characteristic capacitance C_J and critical current I_c , and they are coupled by capacitance C_C . The two degrees of freedom of this system are the phase differences γ_1 and γ_2 , with dynamics governed by the Hamiltonian [8]

$$H = 4E_C(1 + \gamma)^{-1/2}(p_1^2 + p_2^2 + 2\langle p_1 p_2 \rangle) - E_J(\cos \gamma_1 + J_1 \cos \gamma_1 + \cos \gamma_2 + J_2 \cos \gamma_2) \quad (1)$$

Here we have employed the charging and Josephson energies $E_C = e^2/2C_J$ and $E_J = \sim I_c/2e$, the normalized bias currents $J_1 = I_1/I_c$, $J_2 = I_2/I_c$, and the dimensionless coupling parameter $\gamma = C_C/(C_C + C_J)$.

This coupling scheme, recently analyzed by Bulaš et al. [9], Ramos et al. [10], and Johnson et al. [8], results in a system with easily tuned energy levels and adjustable effective coupling. That is, while γ is typically fixed by

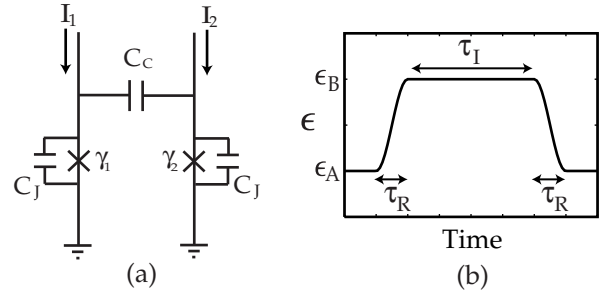


FIG. 1: Capacitively coupled Josephson junctions: (a) ideal circuit diagram; (b) time-dependent ramp of bias currents, specified through the detuning (see text).

fabrication, the energy levels and the effective coupling of the associated eigenstates are under experimental control through J_1 and J_2 . As shown below, the two junctions are effectively decoupled for J_1 and J_2 sufficiently different, but if J_1 and J_2 are related in certain ways, the junctions are maximally coupled. To illustrate this method of control, we define a reference bias current J_0 and consider the variation of J_1 and J_2 through a detuning parameter γ :

$$\frac{p \frac{1}{1 - J_1}}{p \frac{1}{1 - J_2}} = \frac{p \frac{1}{1 - J_0}(1 + \gamma)}{p \frac{1}{1 - J_0}(1 - \gamma)} \quad (2)$$

Quantum logic gates are implemented by varying with time as shown in Fig. 1(b). This ramps the bias currents, moving the system smoothly (with ramp time τ_R) from γ_A , where the eigenstates are essentially unentangled, to γ_B , where the eigenstates are maximally entangled. Entangling evolution is then allowed to occur for an interaction time τ_I , after which the system is ramped back to γ_A .

For analysis, it is convenient to characterize the system by the energy scale $\sim \omega_0 = \sqrt{8E_C E_J (1 - J_0^2)^{1/4}}$ and the effective number N_s of single junction metastable

energy levels when $\epsilon = 0$ [8],

$$N_s = \frac{2^{3=4}}{3} \frac{E_J}{E_C} \stackrel{1=2}{(1 - J_0)^{5=4}} : \quad (3)$$

After choosing a fixed coupling J_0 , gate design requires the identification of suitable N_s , A , B , R , and I . Figure 2 shows the relevant energy levels of H as a function of ϵ for the physically interesting case $J_0 = 0.01$ and $N_s = 4$, and with the potential energy minimum of H subtracted off. The energy levels $E_n(\epsilon)$ and their associated two-junction eigenstates $|j; i\rangle$ were computed using the method of complex scaling [8, 11] applied to the cubic approximation [12] of H .

In general, each energy state $|j; i\rangle$ is an entangled superposition of the product states $|jk; i\rangle$, $j = j_1; i = j_2$, where j_1, j_2 are energy states of an isolated junction with normalized bias current J_1 . (Here we use “round” and “angular” bracket notation to distinguish between coupled and uncoupled bases, respectively.) However, for $j > 0.1$, the energy states are essentially unentangled and well approximated by the product states, which are used to label the corresponding energy levels in Fig. 2. Thus for $A = 0.1$ we find that the eigenstates satisfy the relations $|j; A\rangle = |j0; A i\rangle$, $|j; A\rangle = |j1; A i\rangle$, and $|j; A\rangle = |j1; A i\rangle$. The ground state $|j; i\rangle = |j0; i\rangle$, not shown, remains essentially unentangled for all ϵ . We choose these states for our two-qubit basis. In addition, there are the auxiliary states $|j; A\rangle = |j0; A i\rangle$ and $|j; A\rangle = |j2; A i\rangle$.

For ϵ near $\epsilon = 0.04$ and $\epsilon = 0$, where avoided level crossings occur, we find significant entanglement. Figure 3 shows the entanglement of the states $|j; i\rangle$, with $n = 1; 3; 4; 5$, as a function of ϵ (the entanglement of states 1 and 2 are nearly identical). The entanglement is given in ebits [13]: a state with one ebit entanglement is a maximally entangled two-qubit state. The gates constructed below use this entanglement to perform two-qubit operations.

It is important to take into account the non-qubit states $|j2; i\rangle$ and $|j0; i\rangle$. Poorly designed interactions will result in unwanted evolution of $|j1; i\rangle$ into these auxiliary levels, an effect commonly called leakage. This can be minimized in the following manner. As shown below, at both $B = 0$ and $B = \pi$, the state $|j1; Bi\rangle$ is a superposition of only two of the energy eigenstates. Therefore, its time evolution is oscillatory: $|j1; Bi\rangle \stackrel{iH}{\rightarrow} |j1; Bi\rangle \stackrel{iH}{\rightarrow} |j1; Bi\rangle = a + b \cos^2(\epsilon \tau)$, with $a + b = 1$. Choosing $\tau = k\pi$, where k is an integer, ensures that the oscillation of $|j1; Bi\rangle$ with the auxiliary states completes k full cycles, thus minimizing leakage. This procedure is analogous to quantum logic operations performed in ion traps [14], and allows for stronger coupling than that considered in [9].

If we allow $|j1; i\rangle$ to evolve through states $|j2; i\rangle$ and $|j0; i\rangle$, we must consider another possibility for error.

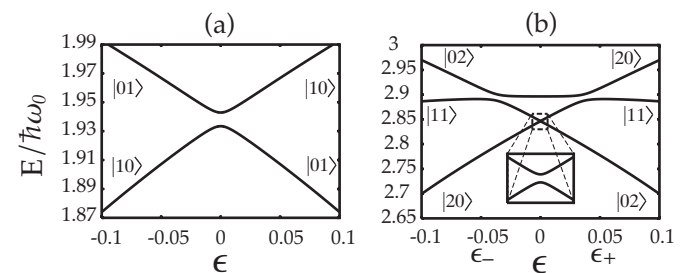


FIG. 2: Normalized energy levels, $N_s = 4$, $J_0 = 0.01$, as a function of detuning parameter ϵ : (a) the energy levels $E_1(\epsilon)$ and $E_2(\epsilon)$ with avoided level crossing at $\epsilon = 0$; (b) the energy levels $E_3(\epsilon)$ through $E_5(\epsilon)$ with avoided crossings of 4 and 5 at $\epsilon = 0$, and 3 and 4 at $\epsilon = 0$.

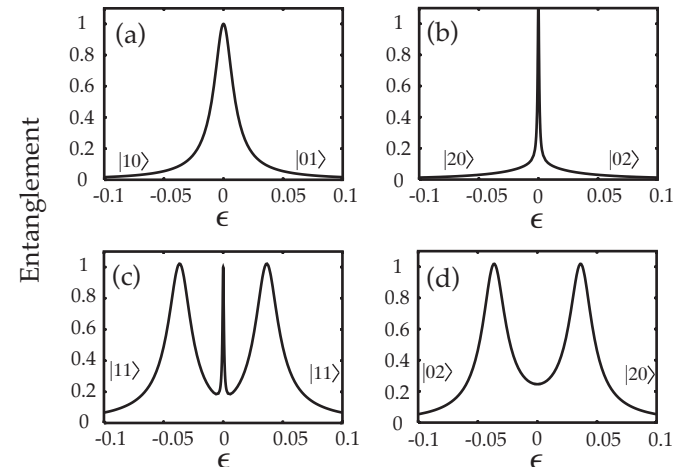


FIG. 3: Entanglement, $N_s = 4$, $J_0 = 0.01$: The entanglement of the energy eigenstates as a function of detuning parameter ϵ : (a) $|j1; i\rangle$; (b) $|j2; i\rangle$; (c) $|j3; i\rangle$; and (d) $|j4; i\rangle$.

That is, the tunneling rates of these auxiliary states are considerably higher than that of $|j1; i\rangle$. We can suppress this tunneling probability by an appropriate choice of N_s : to achieve a fidelity greater than 0.999, our analysis (both numerical and WKB) indicates that the gates should be operated with $N_s = 4$. Finally, we note that proper gate operation requires the rise time τ_R to be adiabatic with respect to single junction energy level spacings, yet nonadiabatic with respect to the coupled energy level splittings. This leads to our choice $\tau_R = 0.01$.

Before analyzing gate dynamics, we look more closely at the eigenstates at $\epsilon = 0$ and $\epsilon = \pi$. These can be understood perturbatively and identified with degeneracies in the combined spectrum of two uncoupled Josephson junctions. For example, with $\epsilon = 0$ at $\epsilon = 0$ the states $|j1; 0i$ and $|j0; 0i$ are degenerate. Coupling splits this

degeneracy [9], and yields the true eigenstates

$$\begin{aligned} |\tilde{1};0\rangle &= 2^{1/2} (|j1;0i - |j0;0i) \\ |\tilde{2};0\rangle &= 2^{1/2} (|j1;0i + |j0;0i). \end{aligned} \quad (4)$$

These states (see Fig. 3(a)) are maximally entangled qubits with an entanglement of 1 ebit. Similarly, states $|j2;0i$ and $|j0;0i$ are degenerate with $= 0$. With nonzero coupling, however, the energy splitting in this case is much smaller [as shown in the inset to Fig 2(b)]. Here, a three-state analysis is required, with the nearly degenerate $|j1;0i$ mediating the coupling. The true eigenstates are approximately

$$\begin{aligned} |\tilde{3};0\rangle &= 2^{1/2} \cos (|j2;0i + |j0;0i) \sin |j1;0i \\ |\tilde{4};0\rangle &= 2^{1/2} (|j2;0i - |j0;0i) \\ |\tilde{5};0\rangle &= 2^{1/2} \sin (|j2;0i + |j0;0i) + \cos |j1;0i; \end{aligned} \quad (5)$$

with $= 0.185$. In accord with Fig. 3(b-d), each of these states is substantially entangled at $= 0$, while $|j1;0i$ is a superposition of $|\tilde{3};0\rangle$ and $|\tilde{5};0\rangle$.

Finally, perturbation theory shows that the α -symmetry degeneracies occur for $= 5=36N_s$. For example, at $= 0$ with $= 0$ states $|j2;0i$ and $|j1;0i$ are degenerate. Coupling leads to the true eigenstates

$$\begin{aligned} |\tilde{4};0\rangle &= 2^{1/2} (|j2;0i - |j1;0i) \\ |\tilde{5};0\rangle &= 2^{1/2} (|j2;0i + |j1;0i). \end{aligned} \quad (6)$$

As seen in Fig. 3(c,d), both eigenstates have an entanglement of 1 ebit. Further, we see that $|j1;0i$ is a superposition of $|\tilde{4};0\rangle$ and $|\tilde{5};0\rangle$.

We can now describe the two-qubit gate that uses the entanglement at α . As noted above, if the state $|j1;0i$ is prepared, its subsequent time evolution (with α held fixed) will be oscillatory. Letting $\tau_1 = 2\pi/\omega_1$, $\tau_2 = 2\pi/\omega_2$, $\tau_3 = 2\pi/\omega_3$, and $\tau_4 = 2\pi/\omega_4$, we find $\tau_1 = \tau_2 = \tau_3 = \tau_4 = \pi/2$. Letting $\tau = \tau_1 = \tau_2 = \pi/2$, we have $\tau_3 = \pi/2 - \tau_1 = \pi/2 - \pi/2 = 0$, and $\tau_4 = \pi/2 - \tau_2 = \pi/2 - \pi/2 = 0$. The remaining states also evolve dynamical phases, which can be factored out as one-qubit gates by letting $U_1 = e^{i\tau_1 R_z(\tau_1)} R_z(\tau_3) e^{iH\tau_3} = e^{i\tau_1 R_z(\tau_1)}$ (as $R_z(\tau_3) = e^{i\tau_3 R_z(\tau_3)}$ is a Pauli matrix). Here $\tau_1 = [\omega_1(0) + \omega_2(0)]\tau_1 = \pi/2$, $\tau_2 = [\omega_1(0) - \omega_2(0)]\tau_2 = \pi/2$, $\tau_3 = [\omega_3(0) - \omega_4(0)]\tau_3 = \pi/2$, and $\tau_4 = [\omega_3(0) + \omega_4(0)]\tau_4 = \pi/2$. A together, in our two-qubit basis, this operation is the controlled-phase gate

$$U_1 = \begin{pmatrix} 0 & & & 1 \\ & 1 & 0 & 0 \\ & 0 & 1 & 0 \\ & 0 & 0 & 1 \\ & 0 & 0 & 0 \end{pmatrix} e^{i\tau_1} \quad (7)$$

with $\alpha = [\omega_4(0) + \omega_0(0) - \omega_1(0) - \omega_2(0)]\tau_1 = \pi/2$. For $N_s = 4$ and $\alpha = 0.01$, we find $\alpha = 1.02$, thus this gate is approximately the controlled-Z gate [15].

We can also use the entanglement at $\alpha = 0$ for quantum logic. From the dynamics of $|j1;0i$ [implied by Eq. 5], we let the interaction time be $\tau_1 = 2\pi/k = [\omega_5(0) - \omega_3(0)]\tau_1 = \pi/2$, where k is an integer. From Eq. (4), however,

the states $|j1;0i$ and $|j0;0i$ will also oscillate [9]. Removing one-qubit dynamical phases as above, we define $U_2 = e^{i\tau_1 R_z(\tau_1)} R_z(\tau_3) e^{iH\tau_3} = e^{i\tau_1 R_z(\tau_1)} R_z(\tau_3) e^{iH\tau_3}$, with $\tau_1 = [\omega_1(0) + \omega_2(0)]\tau_1 = \pi/2$ and $\tau_2 = \tau_3 = [\omega_1(0) + \omega_2(0)]\tau_2 = \pi/2$. For U_2 we find the swap-like gate

$$U_2 = \begin{pmatrix} 0 & & & & 1 \\ & 1 & 0 & 0 & 0 \\ & 0 & \cos \tau_1 & i \sin \tau_1 & 0 & C \\ & 0 & i \sin \tau_1 & \cos \tau_1 & 0 & A \\ & 0 & 0 & 0 & e^{i\tau_2} & \end{pmatrix} \quad (8)$$

with swap angle $\tau_1 = [\omega_2(0) - \omega_1(0)]\tau_1 = \pi/2$ and controlled-phase $\tau_2 = [\omega_5(0) + \omega_0(0) - \omega_1(0) - \omega_2(0)]\tau_2 = \pi/2$. As τ_1 and τ_2 are in general irrational multiples of π , this gate is universal for quantum computation [16]. For example, by tuning J_0 such that $N_s = 5:16$ and letting $k = 2$, the full swap dynamics is generated, with $\tau_1 = \pi/2$, $\tau_2 = \pi/4$, and $\tau_3 = \pi/16$.

Proceeding beyond this heuristic analysis, we have numerically solved the time-dependent Schrödinger equation for H , using the method of split-operator unitary integration [17]. The tunneling dynamics is incorporated through an absorbing boundary condition [18]. Taking $\alpha = 0.1$ as our initial detuning, we have evolved states having initial conditions $|\tilde{4};0\rangle_A, |\tilde{5};0\rangle_A, |\tilde{3};0\rangle_A$, and $|\tilde{2};0\rangle_A$ using the time-dependent Hamiltonian with the ramp function of Fig. 1(b). While the results quoted below are in the cubic approximation, results obtained using the full Hamiltonian (with junction parameters from [2] and [8]) are only marginally different.

The controlled-phase gate U_1 is simulated with $N_s = 4$ and $\alpha = 0.01$. The minimum splitting between $E_4(0)$ and $E_5(0)$ for this N_s is found for $\alpha = 0.036$, and we use this value for ω_B , with $\omega_R = 20\omega_0$ and $\omega_I = 434\omega_0$. The dynamical behavior of this gate is illustrated in Fig. 4(a), where the probability $P(t) = |\langle j4;0 | j(t) | j\rangle|^2$ with $|j(0)\rangle = |\tilde{4};0\rangle_A$ is shown. The computed wave functions at the beginning and middle and end of the evolution, shown in Fig. 5, display the approximate sequence $|j1;0i \rightarrow |j2;0i \rightarrow |j1;0i$. Including all two-qubit states, we find an average gate fidelity [19] $F = 0.996$,

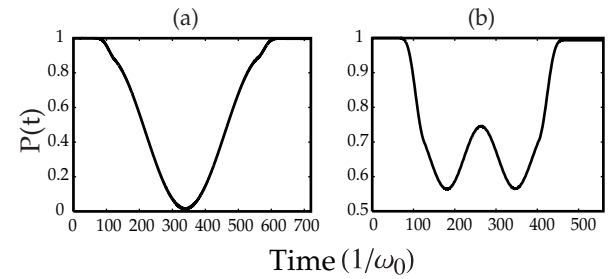


FIG. 4: Dynamical evolution of state with initial condition $|\tilde{4};0\rangle_A$. The probability $P(t) = |\langle j4;0 | j(t) | j\rangle|^2$ is shown for (a) the phase gate U_1 and (b) the swap-like gate U_2 .

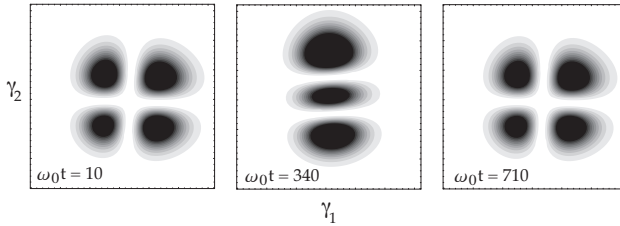


FIG. 5: Dynamical evolution of state with initial condition $j_4; a$) under the phase gate. The contours represent the numerically computed wave function (modulus squared) evolving from what is nearly $j_{11; a}$ through $j_{02; b}$ and back to $j_{11; a}$ with altered phase.

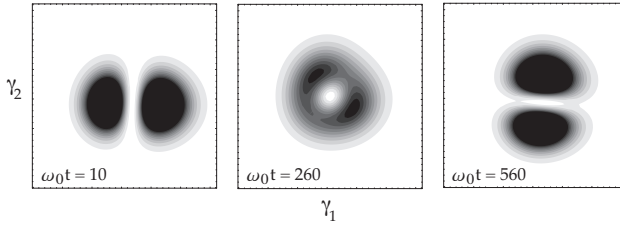


FIG. 6: Dynamical evolution of state with initial condition $j_1; a$) under the swap-like gate. The contours represent the numerically computed wave function (modulus squared) evolving from what is nearly $j_{10; a}$ to $j_{01; b}$ and back to $j_{10; a}$.

with a leakage [20] $L = 0.003$.

For the swap-like gate U_2 , we use $N_s = 5.16$, $\gamma = 0.01$, $\gamma_R = 20 = \gamma_0$ and $\gamma_I = 278 = \gamma_0$. The resulting probability $P(t)$ is shown in Fig. 4(b). The $j_{11; a}$ state completes two oscillations ($k = 2$) but with diminished amplitude due to the shift of the potential minimum, since $j_{11; a} \neq j_{11; b}$ if $\gamma < 1$. The swap of $j_{10; a}$ and $j_{01; b}$ is shown in Fig. 6. This simulated gate is not quite as good as U_1 , with a fidelity $F = 0.972$ and leakage $L = 0.006$. However, we expect that a complete optimization of U_1 and U_2 will yield sufficient fidelity for fault-tolerant quantum computation [21].

A major concern for quantum computing is decoherence. We expect that the swap-like gate U_2 will be susceptible to effects of current noise. As seen in Figs. 3(b,c), the entanglement has a very sensitive dependence on γ . This suggests that fluctuations in γ (caused by current noise) will rapidly drive the $j_{11; a}$ state away from the simple oscillatory dynamics considered above. A realistic optimization of this gate may be difficult, requiring conditions much more elaborate than those constructed above. By contrast, the entanglement near $j_{11; a}$ has a much smoother variation; thus the phase gate U_1 should prove more robust against this source of decoherence.

For both gates, a minimal gate operation time is desirable, but this requires strong coupling. For large γ_R a larger γ_I is required to decouple the junctions. Even

for the case $\gamma = 0.01$ presented here, the eigenstates at $j_{11; a}$ are still somewhat entangled (see Fig. 3). The disadvantage of large detuning is that single-qubit operations may not be possible: for γ too large, the tunneling rates of one junction increase, while the energy levels of the other become more harmonic. Correspondingly, the extension of this scheme to multiple qubits may become problematic.

An attractive solution is the introduction of a middle junction to generate entanglement between adjacent qubits [9]. Specifically, on a state of the form $j_{11} = c_{00}j_{001i} + c_{01}j_{011i} + c_{10}j_{100i} + c_{11}j_{101i}$, the operation $U = (U_2 \otimes I)(I \otimes U_1)(U_2 \otimes I)$ (where I is the one-qubit identity operator) is equivalent (with additional single-qubit operations) to performing a controlled-Z gate on the outermost qubits, leaving the central qubit in the ground state. Since the swap-like gate U_2 never acts on $j_{11; a}$, full optimization of this gate is not necessary and the effect of current noise on this state will be inconsequential.

In conclusion, we have shown how to implement two quantum logic gates in this coupled junction system with time-dependent variations of the bias currents. For U_1 , evolution through auxiliary levels outside of the two-qubit basis generates a controlled phase on state $j_{11; a}$, while for U_2 an additional swap operation is performed between states $j_{01; b}$ and $j_{10; a}$. Finally, we expect that a 3-junction design, using the unitary operations identified here, is an even better candidate for universal quantum computation with capacitively coupled Josephson junctions.

We would like to thank A.J. Berkley, J.M. Martinis, R. Ramos, X. Xu, and M. Gubrud for useful discussions. This work was supported in part by the U.S. Department of Defense and the State of Maryland through the Center for Superconductivity Research.

Electronic address: fstrauch@physics.umd.edu

- [1] R. Ramos et al., IEEE Trans. On Appl. Supercond. 11, 998 (2001).
- [2] J. M. Martinis, S. Nam, J. Aumentado, and C. Urbina, Phys. Rev. Lett. 89, 117901 (2002).
- [3] Y. Yu et al., Science 296, 889 (2002).
- [4] A. J. Leggett, Prog. Theor. Phys. (Suppl) 69, 80 (1980).
- [5] Y. Nakamura, Y. A. Pashkin, and J. S. Tsai, Nature (London) 398, 786 (1999); Y. Makhlin, G. Schon, and A. Shnirman, Rev. Mod. Phys. 73, 357 (2001).
- [6] J. E. Mooij et al., Science 285, 1036 (1999); C. H. van der Wal et al., Science 290, 773 (2000); J. R. Friedman et al., Nature (London) 406, 43 (2000).
- [7] D. Vion et al., Science 296, 886 (2002).
- [8] P. R. Johnson et al., Phys. Rev. B 67, 020509 (2003).
- [9] A. Blais, A. M. Aassen van den Brink, and A. M. Zagoskin, cond-mat/0207112.
- [10] R. C. Ramos et al., IEEE Trans. On Appl. Supercond.

(to appear) (2002).

[11] R. Yariv et al., *Phys. Rev. A* 18, 1816 (1978); E. Caliceti, S. Gra, and M. M. aioli, *Commun. Math. Phys.* 75, 51 (1980).

[12] A. J. Leggett, in *Chance and Matter*, edited by J. Souletie, J. Vannimenus, and R. Stora (Elsevier, Amsterdam, 1987), p. 395.

[13] C. H. Bennett, H. J. Bernstein, S. Popescu, and B. Schumacher, *Phys. Rev. A* 53, 2046 (1996).

[14] J. I. Cirac and P. Zoller, *Phys. Rev. Lett.* 74, 4091 (1995); C. M. Monroe et al., *Phys. Rev. Lett.* 75, 4714 (1995).

[15] M. A. Nielsen and I. L. Chuang, *Quantum Computation and Quantum Information* (Cambridge University Press, 2000).

[16] S. Lloyd, *Phys. Rev. Lett.* 75, 346 (1995).

[17] K. Takahashi and K. Ikeda, *J. Chem. Phys.* 99, 8680 (1993).

[18] R. Kosloff and D. Kosloff, *J. Comput. Phys.* 63, 363 (1986).

[19] M. A. Nielsen, quant-ph/0205035.

[20] R. Fazio, G. M. Palma, and J. Siewert, *Phys. Rev. Lett.* 83, 5385 (1999).

[21] J. Preskill, in *Quantum information and computation*, edited by H.-K. Lo, T. Spiller, and S. Popescu (World Scientific, Singapore, 1998).